A convex reformulation solution approach for the joint perimeter control and route guidance problem

C. Menelaou, S. Timotheou, P. Kolios and C.G. Panayiotou

***Abstract*— Macroscopic traffic management schemes, such as Perimeter Control and Route Guidance, have attracted a lot of attention as primary traffic control strategies for congestion alleviation. Macroscopic methods take advantage of the Macroscopic Fundamental Diagram to capture traffic dynamics within an urban area. Such schemes often result in non-linear and non-convex mathematical programs that are solved with standard non-linear optimization solvers. Nonetheless, non-linear solvers can yield low-quality solutions, are slow and unreliable, and provide no information on the quality of the derived solution. Building upon earlier macroscopic schemes, the contribution of this work is the development of a novel solution methodology for route guidance with perimeter control. The proposed methodology constructs convex outer approximations of all nonlinear constraint sets of the problem to derive: (i) a tight lower bound formulation and (ii) an iterative convexification procedure that provides feasible and upper-bound solutions. The resulting lower and upper bound formulations are solved using Linear Programming producing fast, high quality, and reliable solutions while also providing guaranteed optimality gaps. Macroscopic simulations demonstrate that the proposed methodology executes 2 to 5 times faster than a state-of-the-art non-linear solver and offers an optimality gap of less than 3.9% in all considered cases.**

I. Introduction

Recent advances in communication and vehicle technologies enable the development of a plethora of traffic management schemes that aim to alleviate traffic congestion [1]. For instance, connected vehicles are equipped with onboard units that communicate their speeds and locations to the nearby vehicles and/or network operators. Such technologies enable the emergence of *route guidance* strategies which aim to redistribute traffic away from congested areas by suggesting drivers to follow alternative non-congested routes [2]. Initial developments on route guidance schemes solved the problem by adopting highly detailed and complex microscopic models that require full-state information (such as, the average speed and positions of all vehicles in the network [3]) making their real-life implementation impractical [4].

Recent literature suggests more elegant and efficient way to solve the route guidance problem by employing macroscopic traffic dynamics [5]. According to macroscopic modeling, a road network is partitioned into a set of regions where traffic dynamics are expressed through the concept of the Macroscopic Fundamental Diagram (MFD), [6]. The most significant advantage of MFD modeling is that it allows accurate estimation of the *outflow* of a region, i.e., the rate at which vehicles end their journeys, [4] as validated by [7] using real traffic data. In this context, macroscopic route guidance aims to balance traffic loads across different regions of the network by suggesting different regional paths to drivers at the flow level[8].

Other macroscopic traffic management techniques include *perimeter and gating control* [9], [10]. Perimeter and gating control aim to regulate the transfer flows at the boundaries, i.e., vehicle entries from neighbouring regions, of a protected region to delay and avoid the emergence of congestion within its premises [11]. This is achieved either by managing the traffic signal phases or by applying street closures at the boundaries. Perimeter control is considered as one of the most attractive traffic management schemes. It provides guaranteed closed-loop stability properties [12], [13] and substantially reduced travel times within the protected region [10].

Another advantage of macroscopic approaches is that they can be easily realized within a Model Predictive Control (MPC) framework [14], with the MFD dynamics serving as the prediction model [15]. In this context, different control objectives can be combined, such as the joint perimeter control and route guidance problems [15]. Most macroscopic approaches lead to non-linear and non-convex optimization problems that may yield poor solutions [16]. To anticipate this, works in [17], and [18] reformulate the non-linear MPC problem into a Mixed Integer Linear Program (MILP) using piecewise affine approximation functions. Although such approaches avoid local optima, their real-life implementation is impractical due to the high computational complexity of MILPs. Another approach is to linearise the perimeter control problem by providing traffic state estimates to the MPC scheme [19]. A similar framework was also used in [20], [21] to relax the non-linear route guidance problem. Nonetheless, none of the proposed linearised methods provide any optimality guarantees in terms of solution quality.

This work builds upon previous traffic management strategies that solve the joint route guidance and demand management problem to develop a novel methodology that provides fast, high quality, and reliable solutions, while also providing guaranteed optimality gaps. The proposed framework considers macroscopic dynamics that follow a generalized MFD shape. First, we formulate a tight *lower*

This work has been supported by the European Union's Horizon 2020 research and innovation programme under grant agreement No 739551 (KIOS CoE) , the Government of the Republic of Cyprus through the Directorate General for European Programmes, Coordination and Development and through the Research Promotion Foundation (Project: CULTURE/BR-NE/0517/14).

C. Menelaou, S. Timotheou, P. Kolios and C.G. Panayiotou are with the KIOS Research and Innovation Center of Excellence, and the Department of Electrical and Computer Engineering, University of Cyprus, {cmenel02, timotheou.stelios, pkolios and christosp}@ucy.ac.cy

bound linear mathematical program that is derived based on the convex relaxation of all non-linear constraints. Due to the relaxation of certain constraints, solving the lower bound formulation may yield infeasible solutions; hence, we develop an iterative method that leads to high-quality *upper bound* feasible solutions through the solution of a small number of linear programs. The proposed methodology is compared with a state-of-the-art non-linear solver in terms of optimality gap and computational efficiency. To summarize, the main contributions of this work are:

- We propose a novel convex reformulation of the joint route guidance and perimeter control problem that provides tight *lower bounds* on the optimal solution by relaxing the non-convex constraints of the original problem. Rather than considering a specific MFD shape, we consider generalized flow-density and speed-density MFD shapes.
- For those instances that the resulting solution may be infeasible, we propose a successive convexification method that achieves close-to-optimal *upper bound* solutions to the original problem.

The rest of the paper is organized as follows. Section II presents the multi-regional system model for joint route guidance and perimeter control problem, and Section III formulates the mathematical program of the non-linear MPC framework. Section IV relaxes the problem to a convex program (Lower Bounded solution) and then utilizes the derived control inputs to propose an iterative procedure to produce a feasible solution. Furthermore, Section V includes simulation results and a comparison study of the original non-linear program with the proposed relaxation demonstrating that the proposed approach can offer fast and near-optimal results. Section VI concludes this work and discusses future research directions.

II. Macroscopic Traffic Model

Let an urban area partitioned into $|\mathcal{R}|$ homogeneous regions [22], [23], where $\mathcal{R} = \{1, \dots, |\mathcal{R}|\}$ is the set of all regions and sets $\mathcal{O} \subseteq \mathcal{R}$ and $\mathcal{D} \subseteq \mathcal{R}$ represent the origin and destination regions, respectively. Also, let $\mathcal{J}_r^- \subseteq \mathcal{R}$ denotes the set of neighbouring regions directly adjacent to region $r \in \mathcal{R}$, and similarly let $\mathcal{J}_r^+ = \mathcal{J}_r^- \cup \{r\}$, such that:

$$\mathcal{J}_r = \begin{cases} \mathcal{J}_r^+, \text{ if } r \in \mathcal{D} \\ \mathcal{J}_r^-, \text{ otherwise.} \end{cases} \tag{1}$$

The traffic dynamics within each region $r \in \mathcal{R}$ are defined according to the MFD modeling framework. The time horizon is discretized into time-steps of duration T_s. Let variables $\rho_r(k)$ (veh/km) denote the instantaneous density of vehicles in region $r \in \mathbb{R}$ at time step k, while the parameters ρ_r^J and ρ_r^C denote the *jam* and the *critical* density of region $r \in \mathcal{R}$, respectively [24].

Let also variable $q_r(\rho_r(k))$ (veh/h) denote the *intended outflow* of region $r \in \mathcal{R}$ at time-step k; this variable is equal to the product of density $\rho_r(k)$ (veh/km) and speed $v_r(\rho_r(k))$ (km/h), yielding the relationship

$$q_r(\rho_r(k)) = \rho_r(k) v_r(\rho_r(k)). \tag{2}$$

The term "intended outflow", $q_r(k\rho_r(k)$, indicates the total outflow[1] of region $r \in \mathcal{R}$ when there are no inter-boundary capacity limitations between neighbouring regions. We consider that $q_r(\rho_r(k))$ follows a non-linear generalized MFD shape given by

$$q_r(\rho_r(k)) = f_r(\rho_r(k)), \tag{3}$$

where $f_r(\rho_r(k))$ is a general non-linear function of density (e.g., third order polynomial) [7]. Combining Eqs. (2) and (3) yields

$$v_r(\rho_r(k)) = \frac{f_r(\rho_r(k))}{\rho_r(k)}. \tag{4}$$

Moreover, we introduce parameters L_r and v_r^{MAX} which denote the mean distance traveled by each vehicle and the maximum speed of vehicles in region $r \in \mathcal{R}$, respectively.

To differentiate the portion of traffic destined to different regions, let variable $\rho_{rd}(k)$ indicate the density in region $r \in \mathcal{R}$ towards $d \in \mathcal{D}$, i.e.,

$$\rho_r(k) = \sum_{d \in \mathcal{D}} \rho_{rd}(k). \tag{5}$$

In the same manner, variables $q_{rd}(k)$ and $q_{rjd}(k)$ denote the *intended transfer flow* from $r \in \mathcal{R}$ towards$d \in \mathcal{D}$ and from $r \in \mathcal{R}$ towards$d \in \mathcal{D}$, through neighbouring region $j \in J_r$ at time-step k. Then, it holds true that

$$q_{rjd}(k) = \gamma_{rjd}(k) q_{rd}(k), \tag{6}$$

$$q_{rd}(k) = v_r(k) \rho_{rd}(k), \tag{7}$$

$$q_{rd}(k) = \sum_{j \in \mathcal{J}_r} q_{rjd}(k), \tag{8}$$

$$q_r(\rho_r(k)) = \sum_{d \in \mathcal{D}} q_{rd}(k), \tag{9}$$

$$q_r(\rho_r(k)) = \sum_{d \in \mathcal{D}} \sum_{j \in \mathcal{J}_r} q_{rjd}(k), \tag{10}$$

where variables $\gamma_{rjd}(k) \in [0, 1]$, determine the ratio of vehicles that move from r to d through the adjacent neighbouring region j, such that $\sum_{j \in \mathcal{J}_r} \gamma_{rjd} = 1$, $r \in \mathcal{R}$, $d \in \mathcal{D}$. It is worth mentioning that the flow of vehicles that reach their destination $d \in \mathcal{D}$, meaning that they have completed their journeys at time step k, are indicated by variables $q_{ddd}(k)$, i.e. $q_{rjd}(k)$ for $r = j = d$.

Moreover, variable $C_{rj}(\rho_j(k))$ defines the inter-boundary capacity from region r to neighbouring region $j \in \mathcal{J}_r^-$. The inter-boundary capacity specifies the maximum flow that can be exchanged between the two neighbouring regions expressed as

$$C_{rj}(\rho_j(k)) = \begin{cases} C_{rj}^{\text{MAX}}, \text{ if } \rho_j(k) \leq \beta_{rj} \rho_j^J, \\ \dfrac{C_{rj}^{\text{MAX}}}{1 - \beta_{rj}} \left(1 - \dfrac{\rho_j(k)}{\rho_j^J}\right), \text{ otherwise,} \end{cases} \tag{11}$$

where C_{rj}^{MAX} is the maximum inter-boundary capacity and $\beta_{rj} \rho_j^J$ is the point where the inter-boundary capacity starts to

[1]The total outflow includes the flows that currently are in region $r \in \mathcal{R}$ and are ready to transfer to their neighbours and/or complete their journeys.

decrease with $0 < \beta_{rj} < 1$. Hence, the intended transfer flow is limited by storage capacity of their other neighbouring regions $j \in \{\mathcal{J}_r - r\}$. Thereby, the *actual transfer flow* from $r \in \mathcal{R}$ to $j \in \mathcal{J}_r$ (i.e., $\tilde{q}_{rjd}(k)$), is defined as

$$\tilde{q}_{rjd}(k) = \min\left(q_{rjd}(k), C_{rj}(\rho_j(k))\frac{q_{rjd}(k)}{\sum_{y\in D} q_{rjy}(k)}\right). \tag{12}$$

Taking the above into account, and letting variable $d_{od}(k)$ (veh) denote the number of vehicles that enter in the network from $o \in \mathcal{O}$ towards $d \in \mathcal{D}$ at time-step k (i.e., external demand), then the density traffic dynamics from region $r \in \mathcal{R}$ towards region $d \in \mathcal{D}$ are given by

$$\rho_{rd}(k+1) = \rho_{rd}(k) + \frac{1}{L_r}d_{rd}(k) + \frac{T_s}{L_r}\sum_{j\in\mathcal{J}_r}\big(u_{jr}(k)\tilde{q}_{jrd}(k) - u_{rj}\tilde{q}_{rjd}(k)\big), \tag{13}$$

where, variables $u_{rj}(k) \in [0,1]$ determine the perimeter control actions that regulate the transfer flows between neighbouring regions $r \in \mathcal{R}$ and $j \in \{\mathcal{J}_r - r\}$.

III. Problem Formulation

A. Objective function

Let variables $S^a(k)$ and $S^b(k)$ denote the cumulative number of vehicles that enter the network and successfully arrive at their destination, respectively, defined as

$$S^a(k+1) = S^a(k) + \sum_{o\in\mathcal{O}}\sum_{d\in\mathcal{D}} d_{od}(k),\ k = 1,\, 2, \ldots, \tag{14}$$

$$S^b(k+1) = S^b(k) + T_s\sum_{d\in\mathcal{D}} q_{ddd}(k),\ k = 1,\, 2, \ldots, \tag{15}$$

where $S^a(1) = 0$ and $S^b(1) = 0$.

To define our objective function, we sum over all time-steps the difference between $S^a(k)$ and $S^b(k)$, yielding the Average Time Spent (ATS) of all vehicles in the network, denoted by J_{ATS} (veh·h) and defined as

$$J_{ATS} = T_s\sum_k (S^a(k) - S^b(k)). \tag{16}$$

B. Model Predictive Control Framework

One MPC problem is solved every $M = N^C/T_s$ time-steps where the parameter N^C denotes the control horizon. At a specific time-step $t = M(p-1)$, the measured current states of $\bar{\rho}_r(t)$, $\bar{\rho}_{rd}(t)$ and external demands $d_{rd}(t)$ are used to solve the p-th MPC optimization problem, for the time horizon $\mathcal{K}_p = \{M(p-1)+1, \ldots, M(p-1)+N^P\}$, where N^P denote the prediction horizon, such that $N^P \geq N^C$. The control decisions derived from the proposed MPC framework are the intended transfer flows, $q_{rjd}(k)$ (route guidance), and the perimeter control actions, $u_{rj}(k) \in [0,1]$, $r \in \mathcal{R}$ and $j \in \{\mathcal{J}_r - r\}$ (perimeter control) to minimize the ATS metric by solving the problem:

$$(\mathrm{P}_1)\quad \min\ J^{MPC}_{TTS}(p) = T_s\sum_{k\in\mathcal{K}_p}(S^a(k) - S^b(k)) \tag{17a}$$

s.t. Traffic dynamics: (2) − (15),

$$0 \leq \rho_r(k) \leq \rho^J_r, k \in \mathcal{K}_p, r \in \mathcal{R}, \tag{17b}$$

Initialization: $\rho_r(t) = \bar{\rho}_r(t)$, $\rho_{rd}(t) = \bar{\rho}_{rd}(t)$, $t = M(p-1)$, (17c)

Variables: $\rho_r(k)$, $\rho_{rd}(k)$, $u_{rj}(k)$, $q_r(k)$, $q_{rd}(k)$, $q_{rjd}(k)$, $\tilde{q}_{rjd}(k)$, $v_r(k)$, $S^a(k)$, $S^b(k)$.

In Problem P_1, constraints (2) - (15) model the traffic dynamics according to a generalized MFD shape of Eq. (3). Constraint (17b) ensures that the density of each region is within physical limits, and (17b) defines the initial traffic states. Problem (P_1) is a non-convex Non-Linear Program (NLP) due to the presence of the non-linear unimodal intended outflow function $f_r(\rho_r)$ in Eq. (3), the speed function $v_r(\rho_r)$ in Eq. (4), the bilinear terms in Eqs. (7) and (13), as well as the nonlinear functions in Eq. (11) and Eq. (12).

IV. Convex Solution

In this section we present how Problem (P_1) can be relaxed into a Linear Program (LP) by convexifing all non-convex constraints with convex outer approximation constraints.

A. Lower Bound Solution to Problem P_1

Next, we derive a convex bounding sets for the six non-convex constraints of Problem (P_1), the constraints (3), (4), (7), (11), (12) and (13).

First, to convexify Eq. (3), we form a *convex envelop* of the generalized MFD diagram under density box constraints using piecewise linear segments. Note that box constraints are define within a specified range of density, i.e., $\rho^l_r(k) \leq \rho_r(k) \leq \rho^u_r(k)$, where parameters $\rho^l_r(k)$ and $\rho^u_r(k)$denote the lower and upper bounds of density, respectively. In that regard, we define a set of affine functions of the form, $a_n\rho_r(k) + b_n$, $r \in \mathcal{R}$, $n \in \mathcal{Q}_r(k)$ such that

$$q_r(\rho_r(k)) \leq a_n\rho_r(k) + b_n, \forall n \in \mathcal{Q}_r(k), \tag{18}$$

where $\mathcal{Q}_r(k) = \{1, ..., N_r\}$ is the set of piecewise linear segments that approximate Eq. (3) in region r at time-slot k. Because we are interested in obtaining a lower bound solution, all affine functions are constructed in a way that creates a convex outer approximation set that contains the nonlinear function $f_r(\rho_r(k))$.

Similarly we convexify Eq. (4) by forming a convex envelop of the speed function under density box constraints using piecewise linear segments. Along the same direction we define a set of affine functions of the form, $a_n\rho_r(k)+b_n$, $r \in \mathcal{R}$, $n \in \mathcal{V}_r(k)$ such that

$$v_r(\rho_r(k)) \leq a_n\rho_r(k) + b_n, \forall n \in \mathcal{V}_r(k), \tag{19}$$

where $\mathcal{V}_r(k) = \{1, ..., N_r\}$ is the set of piecewise linear segments defined for the approximation of Eq. (4) in region r at time-slot k.

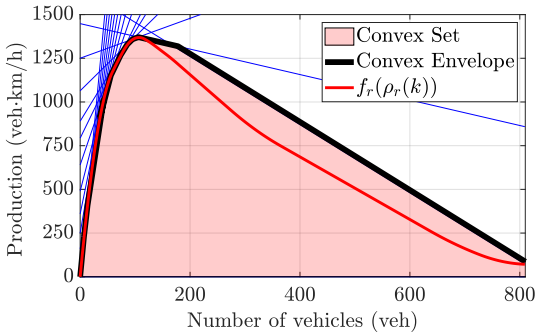

Fig. 1. Example of the bounding set constraints comprised of piecewise linear segments used to derive an outer approximation to the flow MFD relationship given by Eq. (3).

Let us now consider constraint (7) which involves the product of two variables $\rho_{rd}(k)$ and $v_r(\rho_r(k))$. As this constraint has a bilinear term, we use the McCormick method, [25], to derive convex envelopes using the lower and upper bounds of the two variables; in our case it is true that $\rho_r^l(k) \leq \rho_{rd}(k) \leq \rho_r^u(k)$ and $v_r(\rho_r^u(k)) \leq v_r(\rho_r(k)) \leq v_r(\rho_r^l(k))$. The McCormick method approximates (7) with the following four half-spaces:

$$q_{rd}(k) \geq \rho_{rd}(k) v_r(\rho_r^u(k)), \tag{20}$$

$$q_{rd}(k) \geq v_r(\rho_r(k))\rho_r^u(k) + \rho_{rd}(k) v_r(\rho_r^l(k)) - v_r(\rho_r^l(k))\rho_r^u(k), \tag{21}$$

$$q_{rd}(k) \leq v_r(\rho_r(k))\rho_r^u(k), + \rho_{rd}(k) v_r(\rho_r^u(k)) - v_r(\rho_r^u(k))\rho_r^u(k), \tag{22}$$

$$q_{rd}(k) \leq \rho_{rd}(k) v_r(\rho_r^l(k)). \tag{23}$$

Eqs. (20) and (21) are referred to as *underestimators*, while Eqs. (22) and (23) as *overestimators* of Eq. (7). Eqs. (20) - (23) form a convex envelop to the original equality $q_{rd}(k) = \rho_{rd}(k) v_r(\rho_r(k))$, called McCormick envelope, that is a superset of the nonconvex feasibility domain of (7).

Eq. (13) is approximated by

$$\rho_{rd}(k+1) = \rho_{rd}(k) + \frac{1}{L_r} d_{rd}(k) + \frac{T_s}{L_r} \sum_{j \in \mathcal{J}_r} \big((k)\tilde{q}_{jrd}(k) - \tilde{q}_{rjd}(k)\big). \tag{24}$$

Notice that (24) is similar to (13) but with variables $u_{rj}(k)$ removed. This is achieved by letting $\tilde{q}_{rjd}(k)$ take values between 0 and the maximum value as shown later.

Furthermore, constraints (11) and (12) are linearized together according to the procedure proposed in our previous work [26] yielding

$$\tilde{q}_{rjd}(k) \leq q_{rjd}(k), \tag{25}$$

$$\sum_{d \in \mathcal{D}} \tilde{q}_{rjd}(k) \leq C_{rj}^{MAX}, \tag{26}$$

$$\sum_{d \in \mathcal{D}} \tilde{q}_{rjd}(k) \leq \frac{C_{rj}^{\text{MAX}}}{1 - \beta_{rj}} \left(1 - \frac{\rho_j(k)}{\rho_j^J}\right), \tag{27}$$

for all $k \in \mathcal{K}_l$, $r \in \mathcal{R}$, $j \in \mathcal{J}_r$.

Combining all outer approximations of non-convex constraints of Problem P_1 yields

$$(\mathrm{P}_2) \quad \min \; J_{TTS}^{MPC}(l) = T_s \sum_{k \in \mathcal{K}_l} (S^a(k) - S^b(k)) \tag{28}$$

s.t. Constraints: (1), (5), (8) – (10), (14) – (15), (17b) – (17c), (18) – (25), (26) – (27),
Variables: $\rho_r(k)$, $\rho_{rd}(k)$, $u_{rj}(k)$, $q_r(k)$, $q_{rd}(k)$, $q_{rjd}(k)$, $\tilde{q}_{rjd}(k)$, $v_r(k)$, $S^a(k)$, $S^b(k)$.

Formulation (28) is a Linear Program (LP) that provides a lower bound to the optimal solution. Therefore, it can be used to assess the optimality gap of any solution approach for Problem P_1. Formulation (28) may lead to infeasibility, when the solution obtained in the relaxed convex sets violates some of the constraints of Problem P_1. Nonetheless, the split ratios, $\gamma_{rjd}(k)$, and the perimeter control actions, u_{rj}, are implicitly obtained from the solution of Problem P_2. To achieve this, let $q_{rjd}^*(k)$, $q_{rd}^*(k)$ and $q_r^*(\rho_r^*(k))$ denote the obtained flows from the solution of Problem P_2. Then, we define the *split ratio*, $\gamma_{rjd}(k) \in [0,1]$ as

$$\gamma_{rjd}^*(k) = \begin{cases} q_{rjd}^*(k)/q_{rd}^*(k), & \text{for } q_{rd}^*(k) \neq 0, \\ 1/|\mathcal{J}_r|, & \text{for } q_{rd}^*(k) = 0, \end{cases} \tag{29}$$

Similarly, the perimeter control actions, $u_{rj} \in [0,1]$, are defined as

$$u_{rj}^*(k) = \begin{cases} \frac{q_r^*(\rho_r^*(k))}{f_r(\rho_r^*(k))}, & \text{for } q_r^*(\rho_r^*(k)) \neq 0, \\ 0, & \text{for } q_r^*(\rho_r^*(k)) = 0. \end{cases} \tag{30}$$

The next section proposes the *successive ConVexification Route Guidance and Perimeter Control* (CV-RGPC) algorithm that uses the lower bound solution to produce a high quality feasible (upper bound) solution.

B. Successive Convexification Route Guidance and Perimeter Control

In this section we develop a Successive Convexification algorithm for the joint route guidance and perimeter control problem, for obtaining high-quality feasible, upper bound solutions. The CV-RGPC algorithm outlined in Algorithm (1), is a four-step iterative procedure that obtains the decisions of the first M time-steps (split ratios, $\gamma_{rjd}(k)$, and the perimeter control actions, u_{rj}). The key idea of the algorithm is to iteratively tightening the lower and upper bounds of density in each iteration, to achieve convergence to a high quality solution approach.

Initially, the algorithm takes as input, the optimization related parameters, the current state, the traffic parameters, the external demands and initializes the density bounds to their physical limits (Lines: 1-5). Then, a four-step iterative procedure (Lines: 6-12) is executed to obtain feasible solutions of the p-th MPC problem.

Step 1 uses the current density bounds to construct the sets of piecewise linear segments $\mathcal{Q}_r(k)$ and $\mathcal{V}_r(k)$, $r \in \mathcal{R}$, $k \in \mathcal{K}_p$, based on a bisection procedure [27] (Line: 7).

Algorithm 1 Successive Convexification - Route Guidance and Demand Management (CV-RGPC)

Input: Optimization-related parameters: C, N^I N^P, M, p, $t = M(p-1)+1$.
Current state: $\bar{\rho}_r(t)$, $r \in \mathcal{R}$, $\bar{\rho}_{rd}(t)$, $r \in \mathcal{R}$, $d \in \mathcal{D}$, $d_{od}(t)$, $o \in \mathcal{O}$ and $d \in \mathcal{D}$.
Traffic network parameters: $f_r(\rho)$, $g_r(\rho)$, $r \in \mathcal{R}$, C_{rj}^{MAX}, β_{rj}, $j \in \mathcal{J}_r$, $r \in \mathcal{R}$.
, External demands: $d_{od}(k)$, $o \in \mathcal{O}$, $d \in \mathcal{D}$, $k \in \mathcal{K}_p = \{t,\ t+1, \cdots, t+N^P\}$.
Initialization: $\rho_r^l(k) = 0$, $\rho_r^u(k) = \rho_r^J$, $r \in \mathcal{R}$, $k \in \mathcal{K}_p$.
for $\lambda = 1$ to N^I **do**
    Step 1: Derive $\mathcal{Q}_r(k)$ and $\mathcal{V}_r(k)$, $r \in \mathcal{R}$, $k \in \mathcal{K}_p$.
    Step 2: Solve (28) and derive split ratios $\gamma_{rjd}(k)$ and perimeter control actions u_{rj}, $r \in \mathcal{R}$, $j \in \mathcal{J}_r$, $d \in \mathcal{D}$, $k \in \mathcal{K}_p$ using (29).
    Step 3: Use the non-linear traffic dynamics (1) - (15), of Section II and derived future state estimates of densities $\hat{\rho}_r(k)$, $r \in \mathcal{R}$, $k \in \mathcal{K}_p$.
    Step 4: Update bounds on variables $\rho_r(k)$ using Eqs. (31)-(32).
end for
Output: Split ratios $\gamma_{rjd}^*(k)$ and the perimeter control actions u_{rj}^*, $r \in \mathcal{R}$, $j \in \{\mathcal{J}_j - r\}$ and $k \in \mathcal{K}_p$.

Step 2 uses the current bounds on density and solves Problem P_2; then its solution is utilized to compute the split ratios, $\gamma_{rjd}^*(k)$ and the perimeter control actions, $u_{rj}^*(k)$using Eqs. (29) and (30), respectively.

Step 3 takes the derived split ratios and perimeter control actions as input and produces state estimates for the densities of each region, i.e., $\hat{\rho}_r(k)$, $r \in \mathcal{R}$, $k \in \mathcal{K}_p$ by performing simulations (using the non-linear MFD dynamics of Eqs. (1) - (15)) for the whole prediction horizon.

Step 4 uses the state estimates to derive new lower and upper bounds on variables $\rho_r(k)$, $\forall r \in \mathcal{R}$; these bounds are used in Steps 1 and 2 of the next iteration. The upper and lower bounds on variables $\rho_r(k)$ during iteration λ are defined as

$$\rho_r^l(k) = (1 - C_\lambda)\hat{\rho}_r(k),\ \ r \in \mathcal{R},\ k \in \mathcal{K}_p \qquad (31)$$
$$\rho_r^u(k) = (1 + C_\lambda)\hat{\rho}_r(k),\ r \in \mathcal{R},\ k \in \mathcal{K}_p, \qquad (32)$$

respectively, where C_λ is an iteration-dependent constant given by

$$C_\lambda = C\frac{N^I - (\lambda - 1)}{N^I}, \qquad (33)$$

where $C \in (0,1)$ is a constant and N^I is the total number of iterations. Note that on each iteration the density bounds become tighter, and eventually converging in a feasible solution at the end of Step 3 of Algorithm (1).

V. Simulation Results

The proposed methodology is evaluated through macroscopic simulations, where its performance is investigated in terms of computational efficiency and optimality gap compared with the solution of the non-linear program of Problem (P_1) and the case where all vehicles follow their shortest travel time path. In doing so, we consider the 16-regions network as depicted in Fig. 2 in which flows are generated randomly originated from regions 1, 4, 11, and 16 towards regions 2, 8, 9, and 14. Traffic dynamics within each region are based n a third-order polynomial shaped MFD, i.e., $q_r(k) = a_{r_1}\rho_r(k^3) + a_{r_2}\rho_r(k)^2 + a_{r_3}\rho_r(k)$, with the following parameters: $a_{r_1} = 8/1225$, $a_{r_2} = -1192/735$, $a_{r_3} = 14768/147$, $\rho_r^C = 43$ veh/km, $\rho_r^J = 118$ veh/km, $L_r = 1$ km and $q_r^C = 1850$ veh/h, $\forall r \in \mathcal{R}$, $C_{rj}^{\mathrm{MAX}} = 2000$ veh/h, $\beta_{rj} = 0.25$, $\forall r \in \mathcal{R}$, $\forall j \in \mathcal{J}_r$. The simulation time-step, prediction and control horizons are set to $T_s = 30$ s , $N^C = 1$ and $N^P = 10$, respectively.

Region 13	Region 14	Region 15	Region 16
Region 9	Region 10	Region 11	Region 12
Region 5	Region 6	Region 7	Region 8
Region 1	Region 2	Region 3	Region 4

Fig. 2. A simulated urban area consisting of 16 regions.

All schemes are evaluated across different scenarios considering the demand rates of 2300, 3000, 3500, 4000, 4300, and 5000 veh/h. The demand loading procedure holds for an hour and varies across the different O-D pairs. Furthermore, in performed simulations, we assumed that all drivers adhere to the route guidance control inputs, and the boundaries of all considered regions are equipped with traffic lights able to synchronize with the perimeter control actions. For comparison, the performance of the following schemes is examined:

- **SP**: In this scheme, all vehicles follow the shortest travel time path from their origin to their destination.
- **NL**: The solution obtained by solving Problem (P_1) that is solved using the non-linear solver IPOPT [28]. It is worth mentioning that for computational advantages, the inter-boundary capacity constraints, i.e., Eqs. (11) and (12) are omitted from the formulation of Problem (P_1). This reflects the fact that by considering these two constraints, the non-linear solver can not manage to converge within the time limit of 1 hour; similar findings are also discussed in [15].
- **CV-RGPC**: The successive ConVexification Route Guidance and Perimeter Control approach as presented in Section IV-B with the number of iteration set equal with $N^I = 5$ for all simulations that follow. The proposed relaxed problem of Problem (P_2) is solved using the Gurobi mathematical programming solver [29].

		Demand Level (veh/h)					
		2300	3000	3500	4000	4300	5000
ATS (min)	SP	2.7	2.9	3.1	3.4	4.0	4.5
	IPOPT	2.6	2.7	2.8	3.0	3.2	3.3
	CV-RGPC	2.6	2.7	2.8	3.0	3.2	3.3

TABLE I

PERFORMANCE EVALUATION OF DIFFERENT SOLUTION APPROACHES FOR VARYING DEMAND LEVELS.

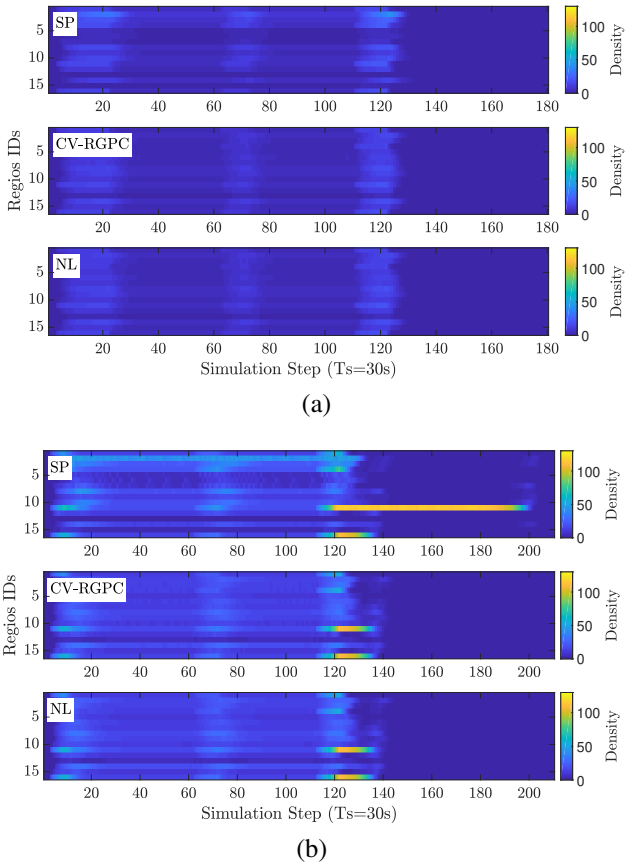

Fig. 3. The instantaneous density of each region observed at each simulation time-step considering (a) 2300 veh/h and (b) 5000 veh/h demand scenarios.

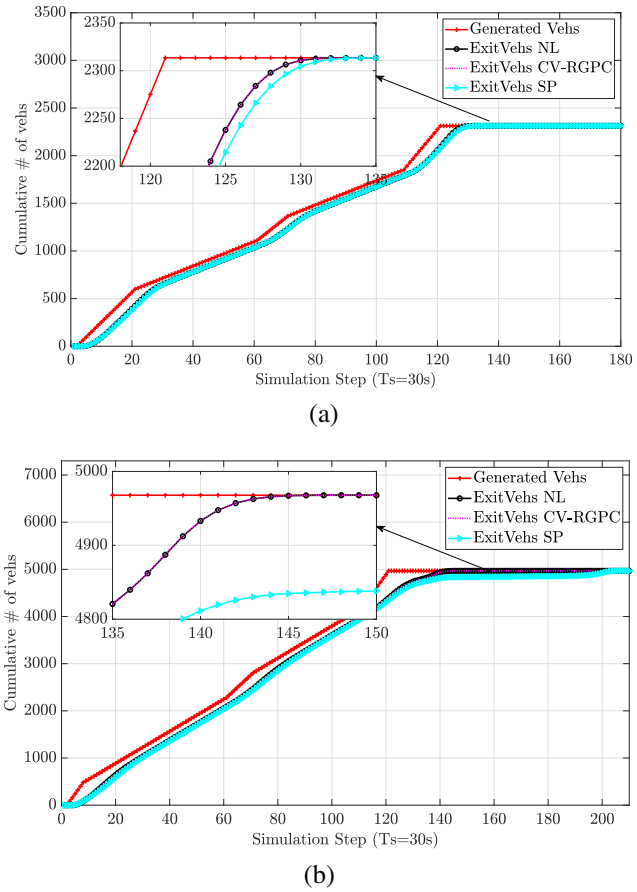

Fig. 4. The cumulative summation of the vehicles number that: i) request to enter the network (Generated Vehs) and ii) exit the network for the SP, NL and CV-RGPC approaches, considering (a) 2300 veh/h and (b) 5000 veh/h demand scenarios.

A. *Performance evaluation*

Table V-A presents the performance results of the three approaches (SP, NL, and CV-RGPC) compared in terms of the Average Time Spent (ATS). As expected, the combination of perimeter and route guidance schemes can lead to significant travel time reductions, especially in high-demand scenarios. More specifically, both CV-RGPC and NL solutions can achieve identical travel times, indicating their excellent performance for all loading scenarios. On the contrary, the SP approach leads to higher travel times where its performance is getting worsen with higher demand rates.

Figs. 3 illustrates the density space-time diagrams for the three approaches considering the demand scenarios of (a) 2300 veh/h and (b) 5000 veh/h. The space-time diagram displays the instantaneous density of each region for the whole simulation duration. In the first scenario, where a relatively lower demand request to be served within the network, all approaches perform equally well. Unlike, in the highest demand scenario, both NL and CV-RGPC manage to serve vehicles in higher flows, and hence improved travel times are observed compared to the SP approach.

Fig. 4 (a) and (b) illustrates the cumulative number of vehicles that request to enter the network (generated) and the number of vehicles that have completed their trips (i.e., exited the network) for the demand scenarios of 2300 veh/h and 5000 veh/h, respectively. Looking at the cumulative number of vehicles that exit the network, the CV-RGPC and NL approaches manage to serve all vehicles faster with enhanced network performance even under the highest demand scenario. From both scenarios, we can observe that when demand is low, all considered approaches perform similarly. In contrast, on higher demands, the joint route guidance and perimeter control approaches can significantly delay and reduce the duration of congested conditions.

Scenario Number	Average Demand	Optimality Gap			
		NL		CV-RGPC	
		Gap	Ex. Time	Gap	Ex. Time
1	2300 veh/h	0.6%	12.1s	0.6%	5.2 s
2	3000 veh/h	1.0%	14.2 s	1.0%	5.2 s
3	3500 veh/h	1.7%	17.7 s	1.7%	5.7 s
4	4000 veh/h	3.0%	14.2 s	3.0%	4.7 s
5	4300 veh/h	4.1%	15.3 s	3.8%	4.4s
6	5000 veh/h	3.8%	22.0 s	3.9%	3.2s

TABLE II

THE OPTIMALITY GAP OF NON-LINEAR PROBLEM AS PRESENTED IN PROBLEM P_1 AND CV-RGPC COMPARED TO THE LOWER BOUND SOLUTION.

B. Optimality Gap and Execution Time

A Lower Bound (LB) solution of the joint route guidance and perimeter control problem can be obtained using formulation (28) with the problem solved once for the entire time horizon, i.e., $\mathcal{K} = \{1, \dots, T + N^P\}$ with $T_s = 30$ s, and $N^C = N^P = 180$. The obtained solution is a LB since there is a discrepancy between the original non-linear problem of the Problem P_1 and the relaxed Problem P_2. On the other hand, the solution obtained from CV-RGPC is an upper bound feasible solution.

To investigate the optimality gap between the two approaches of NL and CV-RGPC with the Lower Bound (LB) solution, we have to compare the optimal objective value obtain from both approaches with the objective function of LB. The optimality criterion of choice is the *optimality gap* defined as follows:

$$\text{Optimality Gap} = \frac{J_{\text{TTS}}^{\text{Alg}} - J_{\text{TTS}}^{\text{LB}}}{J_{\text{TTS}}^{\text{LB}}} \times 100\%,$$

where $J_{\text{TTS}}^{\text{LB}}$ and $J_{\text{TTS}}^{\text{Alg}}$, Alg $= \{$IPOPT , CV-RGPC$\}$, denote the ATS values, according to Eq. (16), obtained from the LB solution and the two solution approaches of IPOPT and CV-RGPC, respectively.

Table II illustrates the optimality gap of the IPOPT and CV-RGPC schemes for all the considered demand scenarios. Both approaches simulated for$T = 120$ min and use the same prediction horizon, time-step and control step duration (i.e., $N_p = 300$ s $T_s = 30$ s and $T_c = 30$s). From the table, we can observe that both CV-RGPC and NL approaches can offer reliable and near to optimality solutions in all cases. More specifically, we can observed that for the case of CV-RGPC at all considered cases the optimality gap is less 4% and almost identical to NL meaning that the proposed solution can offer bounded optimality guarantees. Furthermore, CV-RGPC is 3 to 5 times faster than IPOPT, highlighting that CV-RGPC can offer near optimality solutions significantly faster, even though the constraints of (11) and (12) are omitted from the NL solution.

VI. CONCLUSIONS

This work proposes a novel methodology to solve the joint route guidance and perimeter control problem in which traffic dynamics are defined according to generalized MFDs shapes. The proposed methodology results in a relaxed convex optimization procedure that offers close to optimality results and leads to substantial improvements in network efficiency.

Future research will include a detailed evaluation of the proposed methodology within a microscopic environment and compare it with other state-of-the-art non-MPC schemes (e.g., adaptive control or data-driven approaches). We will also investigate the stability properties of the proposed convex relaxation and develop a robust formulation to deal with uncertainty in modeling, state measurements, and demands.

REFERENCES

[1] M. Papageorgiou, C. Diakaki, V. Dinopoulou, A. Kotsialos, and Y. Wang, "Review of road traffic control strategies," *Proceedings of the IEEE*, vol. 91, no. 12, pp. 2043–2067, 2003.

[2] M. Papageorgiou, "Dynamic modeling, assignment, and route guidance in traffic networks," *Transportation Research Part B: Methodological*, vol. 24, no. 6, pp. 471 – 495, 1990.

[3] H. S. Mahmassani, "Dynamic traffic simulation and assignment: Models, algorithms and application to atis/atms evaluation and operation," in *Operations Research and Decision Aid Methodologies in Traffic and Transportation Management*. Springer, 1998, pp. 104–135.

[4] C. F. Daganzo, "Urban gridlock: macroscopic modeling and mitigation approaches," *Transportation Research Part B: Methodological*, vol. 41, no. 1, pp. 49–62, 2007.

[5] M. Yildirimoglu, M. Ramezani, and N. Geroliminis, "Equilibrium analysis and route guidance in large-scale networks with mfd dynamics," *Transportation Research Part C: Emerging Technologies*, vol. 59, pp. 404–420, 2015.

[6] N. Geroliminis and J. Sun, "Properties of a well-defined macroscopic fundamental diagram for urban traffic," *Transportation Research Part B: Methodological*, vol. 45, no. 3, pp. 605–617, 2011.

[7] N. Geroliminis and C. F. Daganzo, "Existence of urban-scale macroscopic fundamental diagrams: Some experimental findings," *Transportation Research Part B: Methodological*, vol. 42, no. 9, pp. 759–770, 2008.

[8] M. Yildirimoglu and N. Geroliminis, "Approximating dynamic equilibrium conditions with macroscopic fundamental diagrams," *Transportation Research Part B: Methodological*, vol. 70, pp. 186–200, 2014.

[9] M. Keyvan-Ekbatani, A. Kouvelas, I. Papamichail, and M. Papageorgiou, "Exploiting the fundamental diagram of urban networks for feedback-based gating," *Transportation Research Part B: Methodological*, vol. 46, no. 10, pp. 1393–1403, 2012.

[10] N. Geroliminis, J. Haddad, and M. Ramezani, "Optimal perimeter control for two urban regions with macroscopic fundamental diagrams: A model predictive approach," *IEEE Transactions on Intelligent Transportation Systems*, vol. 14, no. 1, pp. 348–359, 2013.

[11] A. Kouvelas, D. Triantafyllos, and N. Geroliminis, "Enhancing model-based feedback perimeter control with data-driven online adaptive optimization," *Transportation Research Part B: Methodological*, vol. 96, pp. 26–45, 2017.

[12] I. I. Sirmatel and N. Geroliminis, "Stabilization of city-scale road traffic networks via macroscopic fundamental diagram-based model predictive perimeter control," *Control Engineering Practice*, vol. 109, p. 104750, 2021. [Online]. Available: https://www.sciencedirect.com/science/article/pii/S0967066121000277

[13] J. Haddad and N. Geroliminis, "On the stability of traffic perimeter control in two-region urban cities," *Transportation Research Part B: Methodological*, vol. 46, no. 9, pp. 1159–1176, 2012.

[14] J. M. Maciejowski, *Predictive control: with constraints*. Pearson education, 2002.

[15] I. I. Sirmatel and N. Geroliminis, "Economic model predictive control of large-scale urban road networks via perimeter control and regional route guidance," *IEEE Transactions on Intelligent Transportation Systems*, vol. 19, no. 4, pp. 1112–1121, April 2018.

[16] M. Hajiahmadi, J. Haddad, B. D. Schutter, and N. Geroliminis, "Optimal hybrid perimeter and switching plans control for urban traffic networks," *IEEE Transactions on Control Systems Technology*, vol. 23, no. 2, pp. 464–478, March 2015.

[17] N. Groot, B. De Schutter, and H. Hellendoorn, "Integrated model predictive traffic and emission control using a piecewise-affine approach," *IEEE Transactions on Intelligent Transportation Systems*, vol. 14, no. 2, pp. 587–598, 2012.

[18] C. Menelaou, S. Timotheou, P. Kolios, and C. Panayiotou, "Joint route guidance and demand management for multi-region traffic networks," in *2019 18th European Control Conference (ECC)*. IEEE, 2019, pp. 2183–2188.

[19] A. Kouvelas, M. Saeedmanesh, and N. Geroliminis, "Linear parameter varying model predictive control for multi-region traffic systems," in *98th Annual Meeting of the Transportation Research Board*. TRB, 2019.

[20] A. Genser and A. Kouvelas, "Optimum route guidance in multi-region networks: A linear approach," in *99th Annual Meeting of the Transportation Research Board*, 2020, pp. 20–30.

[21] C. Menelaou, S. Timotheou, P. Kolios, and C. G. Panayiotou, "Joint route guidance and demandmanagement using generalized mfds," *Appear in Proceedings of IFAC Volumes*, vol. 1, no. 1, 2020.

[22] Y. Ji and N. Geroliminis, "On the spatial partitioning of urban transportation networks," *Transportation Research Part B: Methodological*, vol. 46, no. 10, pp. 1639–1656, 2012.

[23] A. Mazloumian, N. Geroliminis, and D. Helbing, "The spatial variability of vehicle densities as determinant of urban network capacity," *Philosophical Transactions of the Royal Society of London A: Mathematical, Physical and Engineering Sciences*, vol. 368, no. 1928, pp. 4627–4647, 2010.

[24] L. Immers and S. Logghe, *Traffic flow theory*, Lecture Notes, Belgium, May 2003. [Online]. Available: https://www.mech.kuleuven.be

[25] G. P. McCormick, "Computability of global solutions to factorable nonconvex programs: Part i—convex underestimating problems," *Mathematical programming*, vol. 10, no. 1, pp. 147–175, 1976.

[26] C. Menelaou, S. Timotheou, P. Kolios, C. G. Panayiotou, and M. M. Polycarpou, "Path-based joint demand management and route guidance for multi-region traffic networks," in *2019 IEEE Intelligent Transportation Systems Conference (ITSC)*. IEEE, 2019, pp. 3082–3087.

[27] T. H. Cormen, C. E. Leiserson, R. L. Rivest, C. Stein *et al.*, *Introduction to algorithms*. MIT press Cambridge, 2001, vol. 2.

[28] L. T. Biegler and V. M. Zavala, "Large-scale nonlinear programming using ipopt: An integrating framework for enterprise-wide dynamic optimization," *Computers & Chemical Engineering*, vol. 33, no. 3, pp. 575–582, 2009.

[29] Gurobi Optimization Inc., "Gurobi Optimizer Reference Manual," 2016. [Online]. Available: http://www.gurobi.com